electronics

MDPI

Article

Substrate Integrated Waveguide Antenna System for 5G In-Band Full Duplex Applications

Masaud Shah [1], Hammad M. Cheema [1,*] and Qammer H. Abbasi [2]

[1] Research Institute for Microwave and Millimeter-Wave Studies (RIMMS), National University of Sciences and Technology (NUST), Islamabad 44000, Pakistan; mshah.msee17seecs@student.nust.edu.pk
[2] James Watt School of Engineering, University of Glasgow, Glasgow G12 8QQ, UK; Qammer.Abbasi@glasgow.ac.uk
* Correspondence: hammad.cheema@rimms.nust.edu.pk

Abstract: In-band full duplex offers a new approach of meeting the ever-increasing data rate demands by operating the transmitter and receiver at the same frequency at the same time, potentially doubling the spectral efficiency. However, self-interference is the fundamental bottleneck of such systems. In contrast to non-planar or sub 6 GHz microstrip designs reported so-far, this paper presents an all SIW based antenna system for in-band full duplex systems. The proposed design integrates a dual linear polarized three port differential antenna, three port SIW common-mode power combiner and a 180°phase shifter at 28 GHz. Operating the antenna in TE201 mode provides inherent isolation between the differential receive and single-ended transmit port. The residual coupling is further reduced through use of TE101 based power combiner and a 180°phase shifter. Implemented on a 0.508 mm thick RT Duroid 5880 substrate, the antenna occupies a foot-print of 48 $\times$ 80 mm^2. Demonstrating a measured gain of 6.95 dBi and 3.42 dBi for Tx and Rx mode of operation, respectively, the proposed design offers a self-interference cancellation (SiC) of better than 36 dB over a 177 MHz bandwidth.

Keywords: substrate integrated waveguide (SIW); in-band full duplex (IBFD); simultaneous transmit and receive (STAR); self-interference cancellation (SiC); 5G

Citation: Shah, M.; Cheema, H. M.; Abbasi, Q. H. Substrate Integrated Waveguide Antenna System for 5G In-Band Full Duplex Applications. *Electronics* **2021**, *10*, 2456. https://doi.org/10.3390/electronics10202456

Academic Editors: Rafal Przesmycki, Marek Bugaj and Leszek Nowosielski

Received: 18 September 2021
Accepted: 5 October 2021
Published: 10 October 2021

1. Introduction

Global mobile data traffic has experienced an unprecedented growth in the last decade and is projected to be 160 exabyte (EB) per month in 2025. About 76% of this traffic is expected to generate from video that includes streaming services, video advertising and emerging immersive media to name a few [1]. To support these data intensive demands, two general trends are being witnessed. First is the push towards millimeter-wave (mm-wave) frequencies that could address the bandwidth scarcity issue faced at lower frequencies. The second more drastic approach is to re-think the well-known communication architectures so that they could support the data rate requirements of today and beyond. To that end, in-band full duplex (IBFD), an enhancement over full-duplex architecture, enables bidirectional communication at the same carrier frequency and at the same time.

Furthermore, dubbed as simultaneous transmit and receive (STAR), IBFD can double channel efficiency which implies that either the number of users can be doubled within the same bandwidth or the data-rate can be doubled for the same number of users. However, having Tx and Rx at the same carrier frequency results in self-interference (SI) due to direct coupling of Tx signals to the receiver.

The natural consequence is that the receive signals, almost a billion times weaker than the Tx signals, are masked and hence become undetectable. To mitigate this issue, self-interference cancellation (SiC) techniques are adapted that aim at reducing the coupled Tx signal below the receiver noise floor. For instance, a typical bandwidth of 50 MHz, noise figure of 6 dB and transmit power of 27 dBm results in a 120 dB SiC requirement [2]. In an IBFD transceiver, this high value of SiC can only be achieved by dividing it across

three domains, namely the propagation domain which deals with antenna circuitry, analog domain which is composed of Tx and Rx chains, and digital domain which includes the digital signal processors [3].

Achieving higher SiC in propagation domain can relax the requirements down the transceiver's chain and has been a focus of recent research [2,4–17]. One approach utilizes ferrite based circulators to isolate the Tx and Rx; however, they are non-planar and thereby, not aligned with today's miniaturization requirements [14]. Microstrip based planar antennas and circuits constitute the second more common approach; however, most reported designs are limited to sub 6 GHz bands [2,16,17]. Moreover, the contradicting requirements of substrate permittivity for antennas and adjoining cancellation circuits further complicate the design and are prohibitive at mm-wave frequencies. In summary, majority of the reported IBFD designs for propagation domain are non-planar, microstrip based and at sub-6 GHz frequencies.

This paper presents an all integrated SIW antenna system at 28 GHz suitable for IBFD transceivers. SIW provides the benefits of planar integration, low radiation leakage and superior performance at mm-wave frequencies in comparison to microstrip based counterparts. As shown in Figure 1, the proposed design consists of a differential antenna, a three port common-mode power combiner and a 180°phase shifter interconnected all through SIW. The Tx leakage (represented by black dashed lines) that is coupled to the two Rx paths is in-phase to each other. Passing one arm through a 180° phase shifter and subsequent power combining, results in their cancellation, thus minimizing the effect of coupled Tx signals. On the other hand, when one of the differential receive signal (represented by green color) is passed through the 180° phase shifter, it becomes in-phase to the other and constructively adds at the power combiner. The final integrated antenna offers 6.95 for port 1 (Tx) and 3.42 dBi gain for port 2 (Rx). In a foot-print of 48 $\times$ 80 mm^2, the proposed system achieves SiC of better than 36 dB over 177 MHz bandwidth.

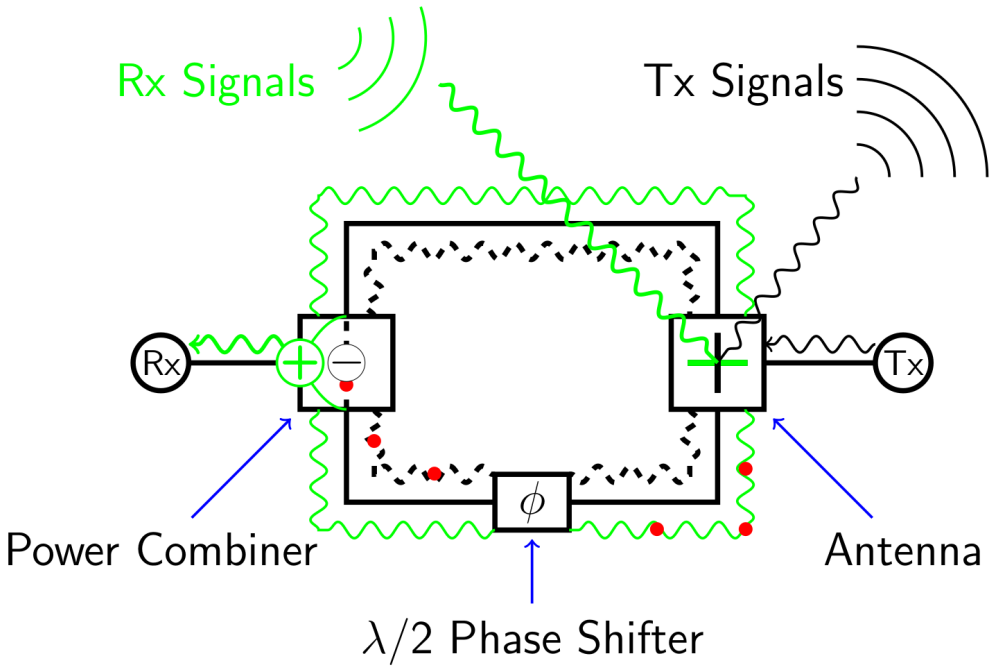

Figure 1. Proposed SIW antenna system operation [red dot represent the out of phase component].

The remaining paper is organized as follows. Section II and III discusses the proposed three port SIW differential antenna and three port common mode SIW power combiner, respectively. Section IV presents the combined antenna system followed by conclusions in Sections V, VI, and VII.

2. SIW Differential Antenna

The antenna requirements outlined in Figure 1 include differential operation in Rx mode, single-ended operation in Tx mode with a preferable intrinsic isolation mechanism between them. To that end, various SIW modes were studied and TE201 mode was chosen for the SIW antenna. As illustrated in Figure 2a, this mode under port 1 (Tx) excitation, provides minimum in-phase coupling to port 2 and port 3, which cancel through power combiner, thus offering inherent isolation between the Tx and Rx ports. Similarly, when Rx signals impinge upon the antenna (Figure 2b), the electric fields are out-of-phase to each other at port 2 and 3 with minima at port 1. Operating port 2 and port 3 of antenna in differential manner enable the extraction of Rx signals. Finally, orthogonal radiation slots are used as shown in Figure 2 to further support the radiation under TE201 mode. Under Tx operation, the slot perpendicular to Tx feed line radiates while the parallel slot does not radiate and the opposite is true for Rx operation.

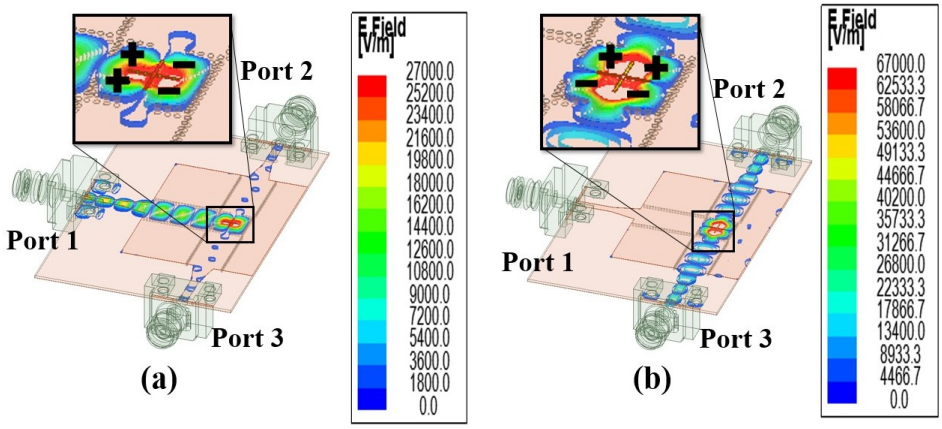

Figure 2. Modes (electric field) intensity for antenna at 28 GHz, (**a**) single-ended excitation from port 1, (**b**) differential excitation from port 2 and port 3 [red and blue show highest and lowest intensity, respectively].

As part of the design evolution, first an SIW cavity was designed for the desired TE201 mode according to [18,19]. The initial frequency of 34 GHz is chosen as the subsequent introduction of slot reduces the resonance frequency to the intended 28 GHz. Next an SIW feed line (single-ended for Tx) and a $\lambda/2$ radiation slot (with respect to 28 GHz) perpendicular to feed line was added. The cavity opening towards the feed line was also created through removal of adequate number of Vias (Figure 3a). At this point the antenna results were analyzed to achieve optimum performance at 28 GHz. As a next step, for the differential Rx side, two SIW feed lines were added perpendicular to the Tx feed line and a second radiation slot was also added in the cavity, perpendicular to first slot. Cavity openings towards these new feed lines also included (Figure 3b). Parametric study was carried out to get optimum results for single-ended as well as differential excitation. Finally, SIW to microstrip transition and tapering for the connector was included to complete the design.

The simulated mixed mode S-parameters of the antenna, including 2.92 mm connector model, are extracted as per [20] and shown in Figure 4. *Sdd* represents differential matching of antenna for port 2 and port 3 and yields a bandwidth of 400 MHz. *S*11 represents single ended matching whereas *Scc* represents common mode matching for port 2 and port 3. The latter being -1.3 dB verifies that common mode signals cannot excite the antenna. Lastly, *S*1*d* represents the inherent self-interference cancellation for the antenna alone.

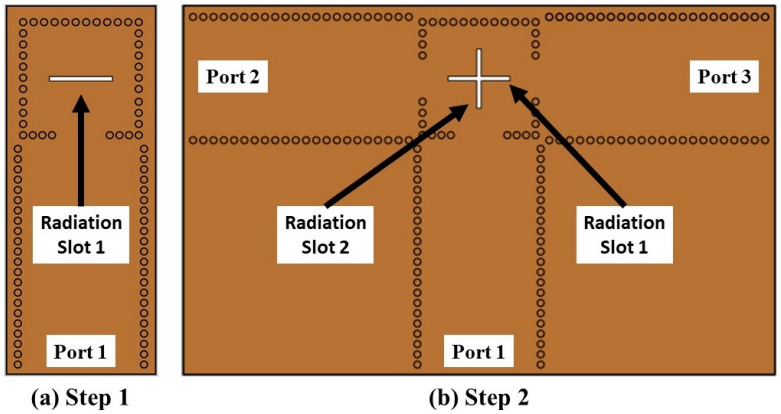

Figure 3. Design evolution of SIW antenna, (**a**) design of cavity, single-ended feed and radiation slot 1, (**b**) design of differential feed and radiation slot 2.

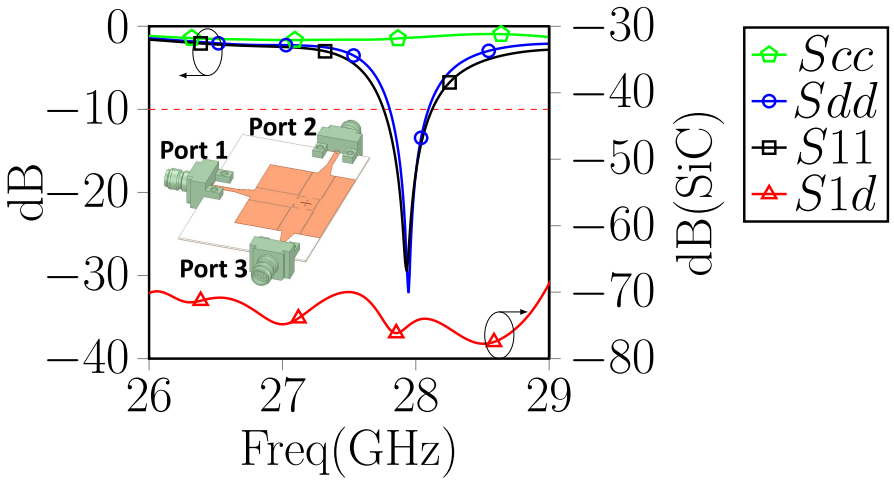

Figure 4. S-parameters of SIW differential antenna.

3. SIW Power Combiner

A few conventional designs have utilized rat-race couplers in conjunction with an antenna to achieve self-interference cancellation. However, this approach either results in interconnection complexity or the fourth port being dormant [2,17]. In contrast, the proposed SIW power combiner directly interconnects with the antenna simplifying the design considerably.

It utilizes TE101 mode that is characterized either by positive or negative electric fields inside the cavity at a single time. Inherently, a TE101 mode based cavity adds in-phase signals and cancels out-of-phase signals. However, as opposite functionality is required from the proposed power combiner, a $\lambda/2$ line is added to one arm (port 3). In other words, the power combiner adds out-of-phase signals and cancels in-phase signals as confirmed in Figure 5.

The simulated mixed mode S-parameters of power combiner with $\lambda/2$ line are shown in Figure 6. *Sdd* represents differential matching of the power combiner's port 2 and port 3 and exhibit a 1.9 GHz bandwidth whereas *S*11 represents single-ended matching of port 1. *Scc* is the common-mode matching for port 2 and port 3 and its value is ≈ -0.9 dB. *S*1*d* represents the combined signal at port 1 under 180°-out-of-phase excitation of port 2 and port 3, and corresponds to an insertion loss of ≈1.45 dB. Finally, *S*1*c* represents the cancellation of signals under same-phase excitation of port 2 and port 3 and its peak value is >47 dB.

Since Rx signals from the proposed antenna are out-of-phase and Tx leakage is in-phase at port 2 and port 3, the proposed power combiner (with $\lambda/2$ line) will extract

the desired Rx signals and cancel the Tx leakage as verified through field propagation (Figure 5) and S-parameters (Figure 6).

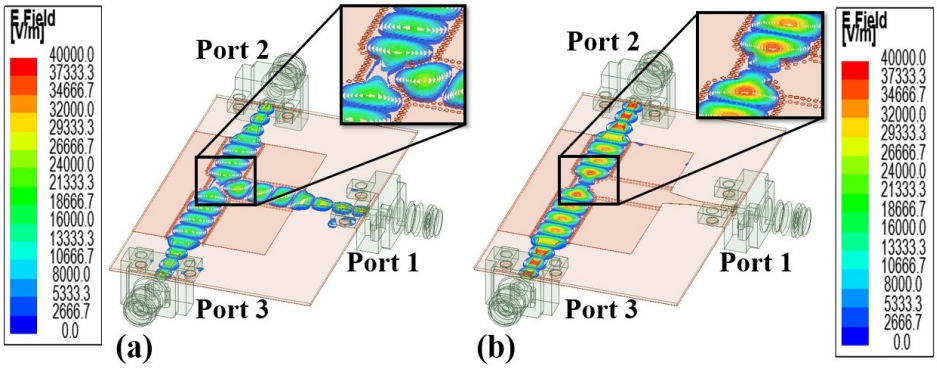

Figure 5. Modes (electric field) intensity for power combiner with $\lambda/2$ line, (**a**) 180° out-of-phase excitation of port 2 and port 3 (**b**) In-phase excitation of port 2 and port 3 [red and blue show highest and lowest intensity, respectively].

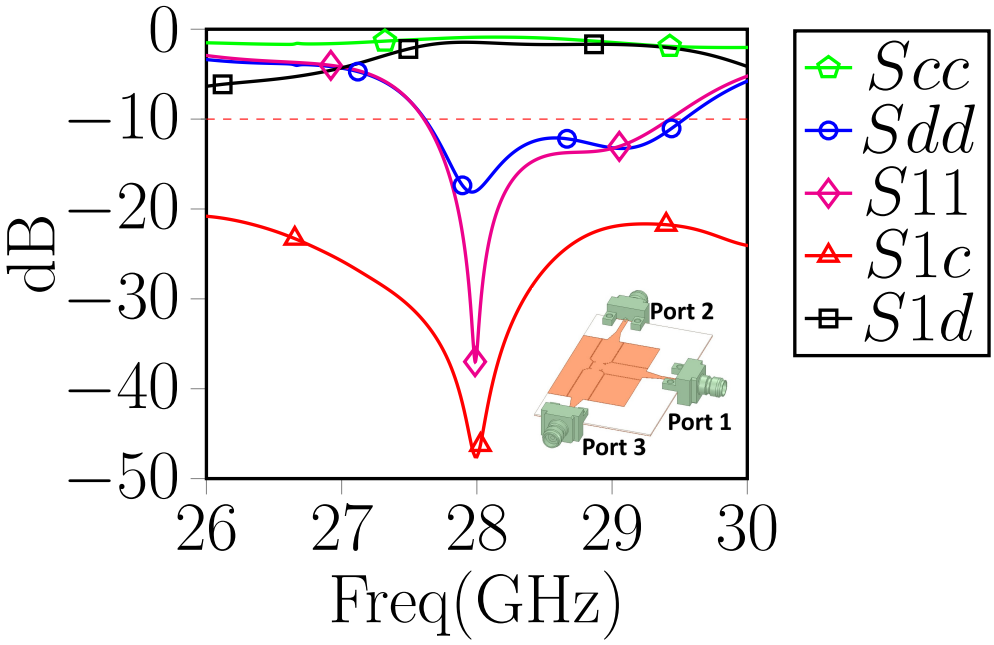

Figure 6. S-parameters of SIW power combiner with $\lambda/2$ SIW line.

4. Combined Antenna System

The final step in the IBFD antenna system design included interconnection of the antenna and power combiner through SIW. For this purpose, U-shaped bends were utilized and separately designed and characterized. The measured results of these bends are shown in Figure 7 and show good match with simulations.

The complete SIW antenna system is shown in Figure 8. In order to have a symmetric design, the required 4.24 mm (equivalent to $\lambda/2$) in one arm of the SIW antenna system is divided into two 2.12 mm offsets towards $+z$ and added to the power combiner. The fields inside combined antenna system are shown in Figure 9.

The combined antenna system was designed using RT / duroid 5880 with substrate height 0.508 mm and copper thickness of 0.035 mm. The detailed dimensions (in millimeter) of SIW antenna system are l 47.96, ww 53.79, w 80.31, d 0.4, mw 1.65, stw 4, ml 6.73, stl 5.26, ctw 0.9, ctl 1.27, cgo 0.8, cgl 5.5, cgvo 2, a 7.2, p 0.6, cgw 0.508, sw 0.2, ac 6.6, sltx 3.54, slrx 3.41, os 3.3, od 2.7, acp 4.19, osp 3.39, odp 2.99, mwp 1.52.

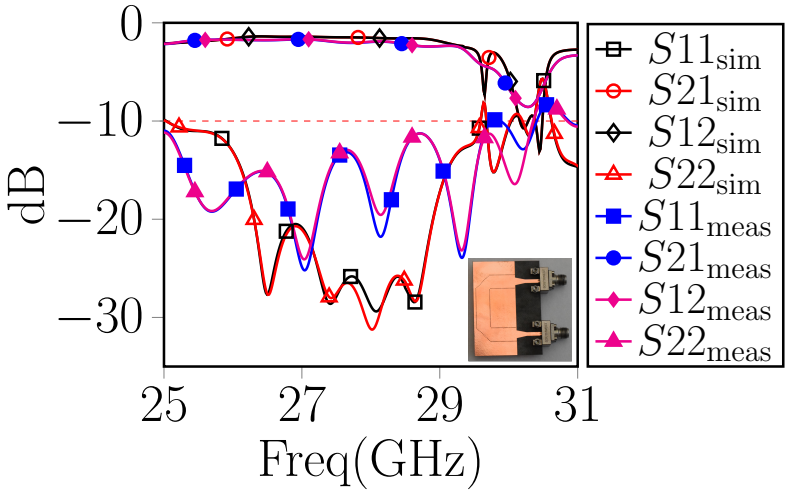

Figure 7. U-shaped bend s-parameters.

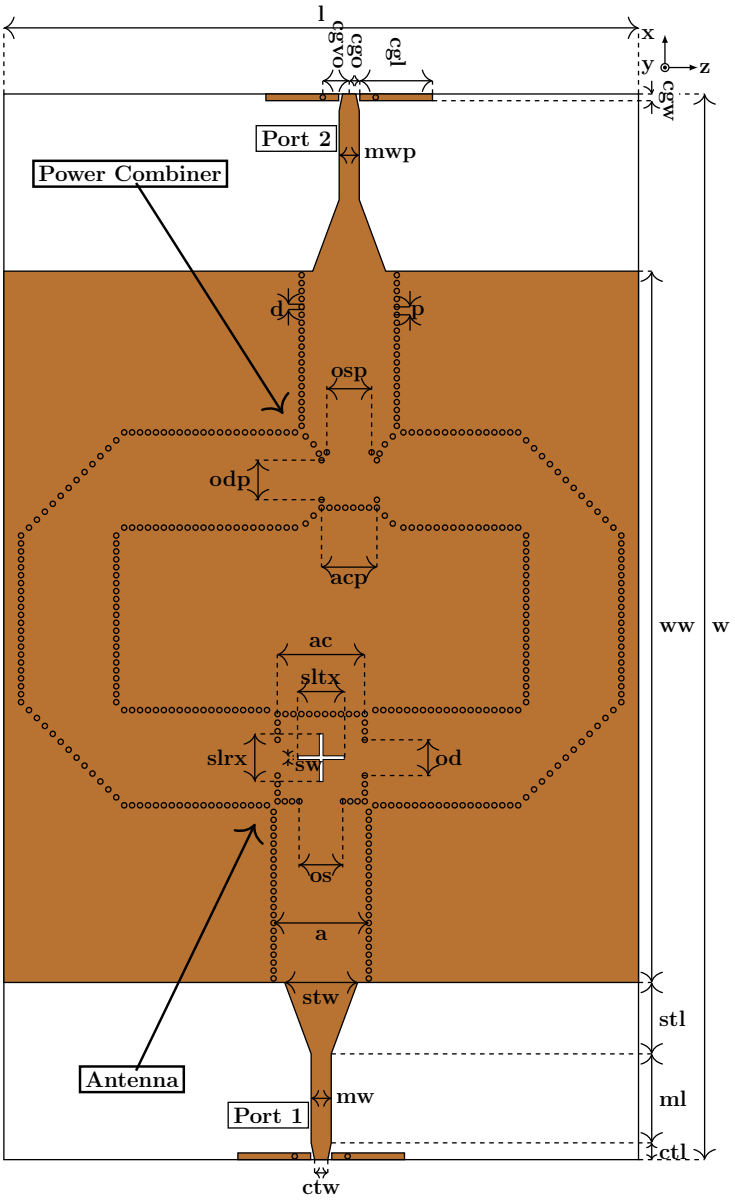

Figure 8. Dimensional view of SIW antenna system.

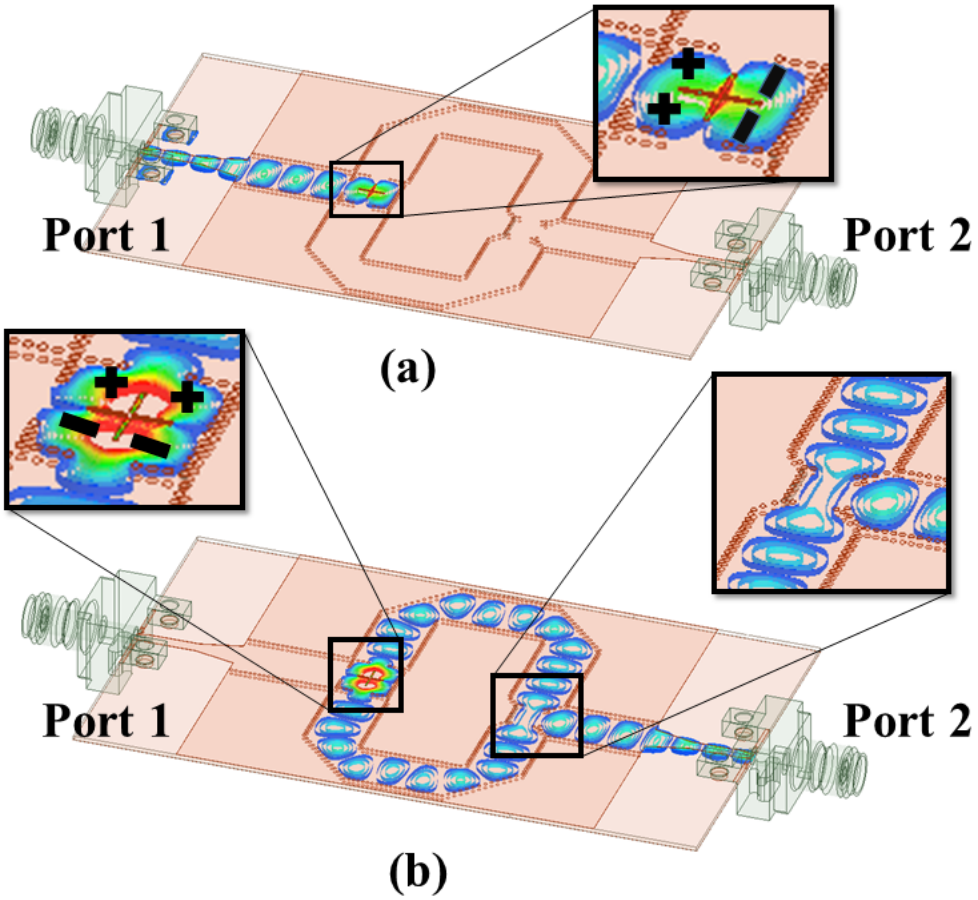

Figure 9. Modes (electric field) intensity for combined antenna system at 28 GHz, (**a**) excitation from port 1, (**b**) excitation from port 2 [red and blue show highest and lowest intensity, respectively].

5. Measurement Results

The fabricated antenna is shown in Figure 10 along with measurement setup pictures. The S-parameters are measured using Anritsu MS46122B VNA and shown in Figure 11. *S*11 and *S*22 represent matching for port 1 (Tx) and port 2 (Rx), respectively, while *S*12 (or *S*21) represents the key SiC parameter. In comparison to the simulated 42 dB at resonance frequency of 28 GHz, the measured SiC is better than 36 dB at 27.64 GHz. In order to identify the reason of slightly lower than expected SiC, post measurement simulations using the S-parameters (.s3p files) were done in Keysight's Advanced Design System in a configuration similar to Figure 1. The phase difference between one arm was varied and the result is shown in Figure 12. It can be observed that when the phase difference is exactly 180°, 60 dB SiC over the band with peak SiC of >80 dB can be achieved. The SiC, when plotted for 175°, 185°, and 190° shows that similar numbers can be achieved but are shifted in each case. Therefore, the measured SiC of ≈53 dB corresponding to 28.36 GHz is when the exact phase shift of 180° is obtained (Figure 11). Conversely, at best matching frequency of 27.64 GHz, the obtained phase difference is not exactly 180°due to which a lower SiC of 36 dB is achieved (Figure 11). This indicates the need of alternatives to the adopted length based phase shifters that are prone to ±10% variation [21].

The radiation patterns were measured in NSI far-field anechoic chamber and show good matching between simulations and measurements (Figure 13). The gain for port 1 (Tx) is 6.95 dBi and for port 2 (Rx) is 3.42 dBi. The front-to-back-ratio (FBR) for port 1 and port 2 are −19 dB and −8 dB, respectively, while cross-polarization ratio for port 1 and port 2 are −17 dB and −6 dB, respectively. The lower port 2 values of gain, FBR, and cross polarization are also attributed to the earlier explained tolerances in the length based phase shifter.

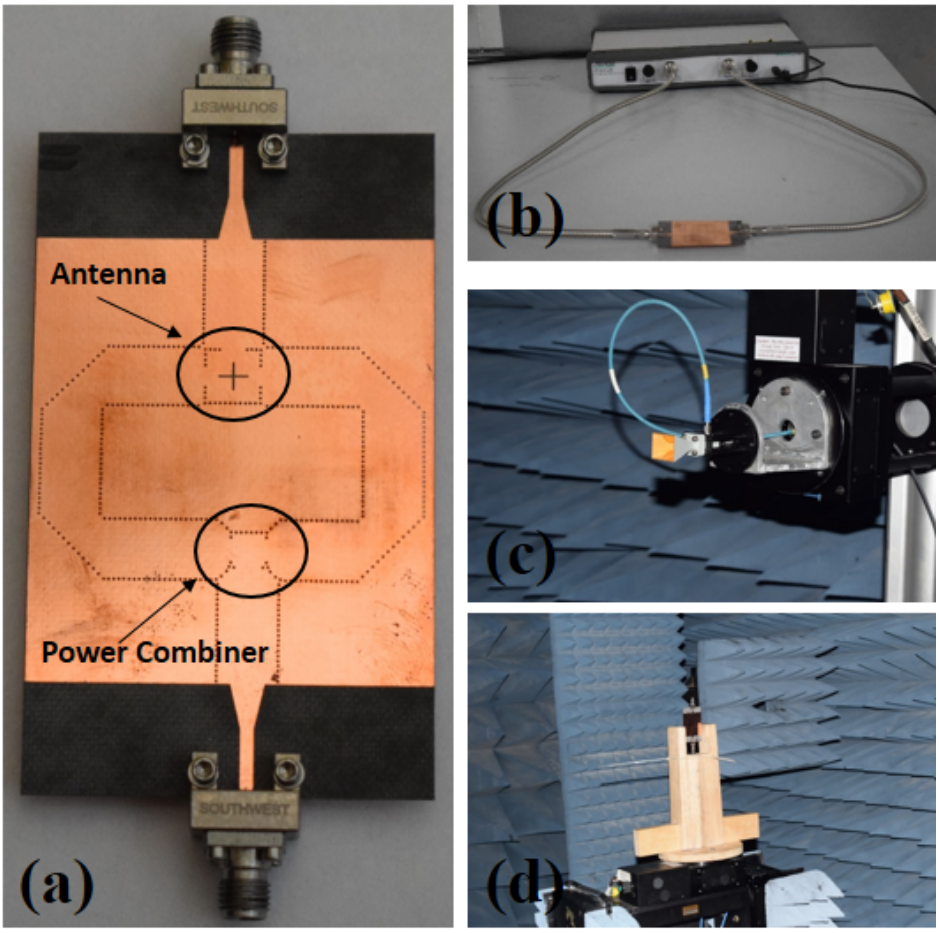

Figure 10. (**a**) SIW antenna system, (**b**) SIW antenna system with VNA, (**c**) standard gain antenna, (**d**) SIW antenna system in anechoic chamber.

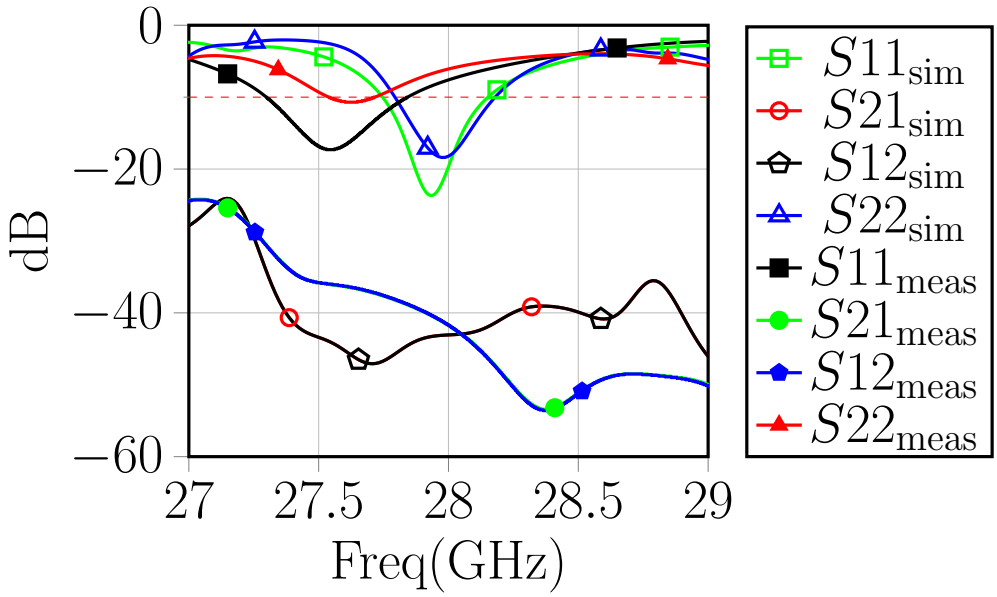

Figure 11. S-parameters of SIW antenna system.

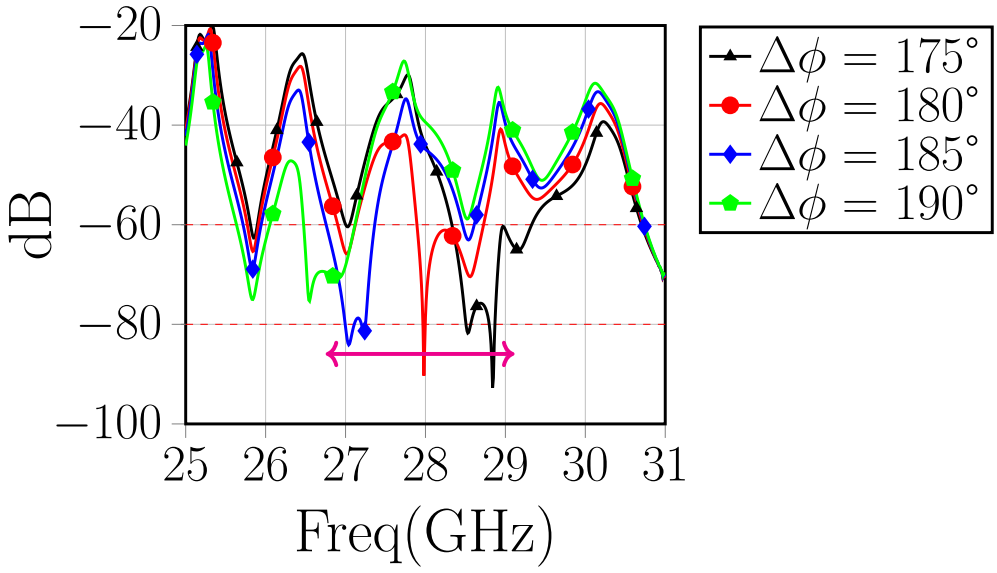

Figure 12. SiC dependence on phase shift in the SIW integrated antenna.

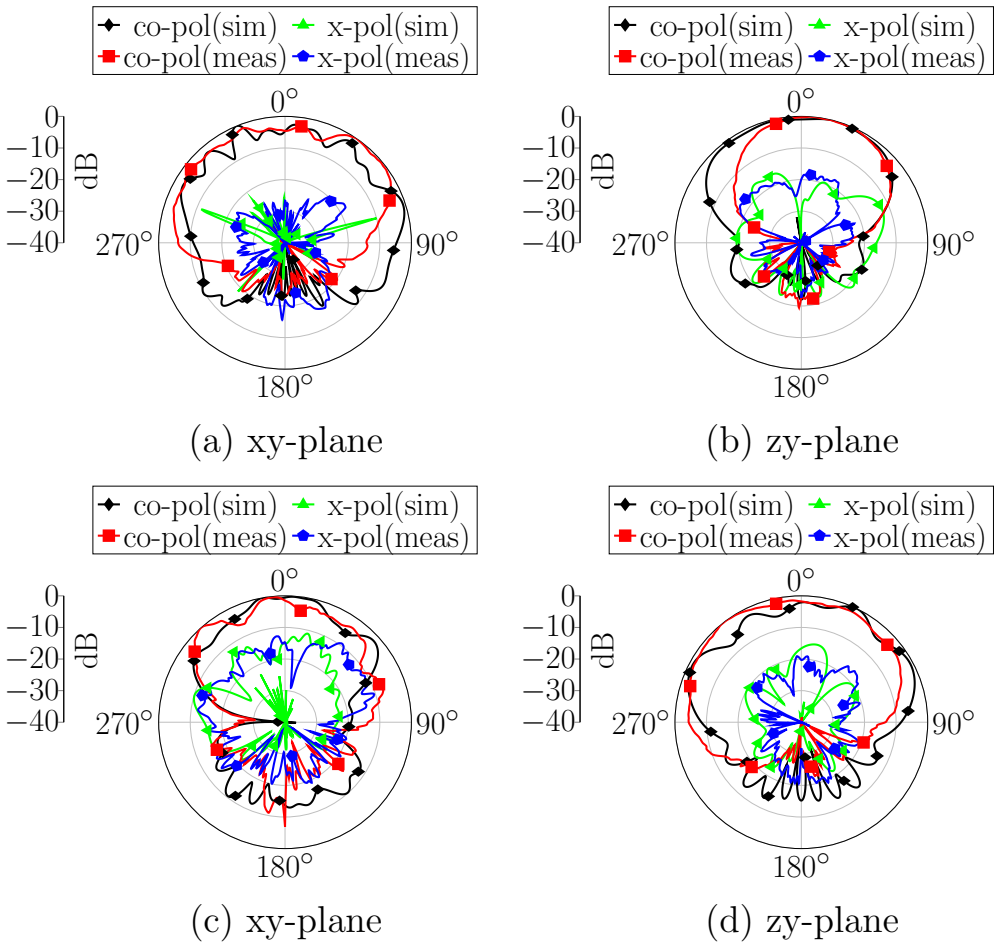

Figure 13. Radiation pattern of SIW integrated antenna, (**a**,**b**) represent port 1, (**c**,**d**) represent port 2.

6. Comparison with Recent Work

The comparison of this work to recent microstrip based IBFD designs is shown in Table 1. It is evident that all designs are sub 6 GHz and some only report the antenna without the interconnection mechanism. To the best of author's knowledge, the presented

work is one of the first SIW IBFD antenna system for 5G applications at 28 GHz that provides a simpler alternative to the reported designs with favorable SiC performance.

Table 1. Comparison with published works.

Ref. & Year	Comments	Freq. (GHz)	Fractional BW. (%)	Peak SiC (dB)
[16] 2019	4 Patch Antennas with Complex Feed	2.45	4.08	54
[17] 2019	Microstrip Based Proximity Fed 4 patch Antennas	3.5	2.31	>50
[2] 2017	Planar Microstrip Integrated Differential Antenna With Feed	2.4	2.08	67
[22] 2020	Double Differential Patch Antenna Only	4.9	6	>33
This Work	Planar SIW Integrated Antenna System	28	0.63	>36

7. Conclusions

An all SIW based antenna system for in-band full duplex communication was presented. The proposed design integrates a dual linear polarized three port differential antenna, three port SIW common-mode power combiner and a 180°phase shifter at 28 GHz. Utilizing specific modes for the antenna and power combiner, the achieved peak self-interference cancellation is >36 dB. In foot-print of 48 × 80 mm^2, the antenna system offers a gain of 6.95 dBi in the Tx mode and 3.42 dBi in the Rx mode. The planar design with cancellation mechanism makes it suitable for future 5G IBFD systems.

Author Contributions: Data curation, M.S.; Investigation, M.S.; Methodology, M.S. and H.M.C.; Resources, Q.H.A.; Writing—review & editing, M.S, H.M.C. and Q.H.A. All authors have read and agreed to the published version of the manuscript.

Funding: This work is supported in parts by EPSRC grant reference number EP/R511705/1.

Data Availability Statement: Data are contained within the article.

Acknowledgments: Authors would like to acknowledge Mudassir Ali and Muhammad Zeeshan for their assistance in performing the measurements.

Conflicts of Interest: The authors declare no conflict of interest.

References

1. Mobile Traffic by Application Aategory. Available online: https://www.ericsson.com/en/mobility-report/reports/november-2019 (accessed on 21 April 2020).
2. Nawaz, H.; Tekin, I. Dual-Polarized, Differential Fed Microstrip Patch Antennas With Very High Interport Isolation for Full-Duplex Communication. *IEEE Trans. Antennas Propag.* **2017**, *65*, 7355–7360.
3. Kolodziej, K.E.; Perry, B.T.; Herd, J.S. In-Band Full-Duplex Technology: Techniques and Systems Survey. *IEEE Trans. Microw. Theory Tech.* **2019**, *67*, 3025–3041.
4. Shah, M.; Cheema, H.M. SIW Antenna for 5G In-Band Full Duplex Applications. In Proceedings of the 2020 IEEE International Symposium on Antennas and Propagation and North American Radio Science Meeting, Atlanta, GA, USA, 7–12 July 2020; pp. 331–332. doi:10.1109/IEEECONF35879.2020.9330371.
5. Zhang, Y.; Li, J. Differential-Series-Fed Dual-Polarized Traveling-Wave Array for Full-Duplex Applications. *IEEE Trans. Antennas Propag.* **2020**, *68*, 4097–4102.
6. Ye, L.H.; Zhang, X.Y.; Gao, Y.; Xue, Q. Wideband Dual-Polarized Four-Folded-Dipole Antenna Array With Stable Radiation Pattern for Base-Station Applications. *IEEE Trans. Antennas Propag.* **2020**, *68*, 4428–4436.
7. Wu, D.; Sun, Y.; Wang, B.; Lian, R. A Compact, Monostatic, Co-Circularly Polarized Simultaneous Transmit and Receive (STAR) Antenna With High Isolation. *IEEE Antennas Wirel. Propag. Lett.* **2020**, *19*, 1127–1131.
8. Sun, L.; Li, Y.; Zhang, Z.; Feng, Z. Compact Co-Horizontally Polarized Full-Duplex Antenna With Omnidirectional Patterns. *IEEE Antennas Wirel. Propag. Lett.* **2019**, *18*, 1154–1158.
9. Etellisi, E.A.; Elmansouri, M.A.; Filipovic, D.S. Wideband Monostatic Co-Polarized Co-Channel Simultaneous Transmit and Receive Broadside Circular Array Antenna. *IEEE Trans. Antennas Propag.* **2019**, *67*, 843–852.

10. Abdelrahman, A.H.; Filipovic, D.S. Antenna System for Full-Duplex Operation of Handheld Radios. *IEEE Trans. Antennas Propag.* **2019**, *67*, 522–530.
11. Zhang, Y.; Zhang, S.; Li, J.; Pedersen, G.F. A Dual-Polarized Linear Antenna Array With Improved Isolation Using a Slotline-Based 180° Hybrid for Full-Duplex Applications. *IEEE Antennas Wirel. Propag. Lett.* **2019**, *18*, 348–352.
12. Khaledian, S.; Farzami, F.; Smida, B.; Erricolo, D. Robust Self-Interference Cancellation for Microstrip Antennas by Means of Phase Reconfigurable Coupler. *IEEE Trans. Antennas Propag.* **2018**, *66*, 5574–5579.
13. Zhang, Y.; Li, J. An Orbital Angular Momentum-Based Array for In-Band Full-Duplex Communications. *IEEE Antennas Wirel. Propag. Lett.* **2019**, *18*, 417–421.
14. Khaledian, S.; Farzami, F.; Smida, B.; Erricolo, D. Inherent Self-Interference Cancellation for In-Band Full-Duplex Single-Antenna Systems. *IEEE Trans. Microw. Theory Tech.* **2018**, *66*, 2842–2850.
15. Etellisi, E.A.; Elmansouri, M.A.; Filipovic, D.S. Wideband Monostatic Simultaneous Transmit and Receive (STAR) Antenna. *IEEE Trans. Antennas Propag.* **2016**, *64*, 6–15.
16. Zhou, Z.; Li, Y.; Hu, J.; He, Y.; Zhang, Z.; Chen, P. Monostatic Copolarized Simultaneous Transmit and Receive (STAR) Antenna by Integrated Single-Layer Design. *IEEE Antennas Wirel. Propag. Lett.* **2019**, *18*, 472–476.
17. Deng, C.; Yektakhah, B.; Sarabandi, K. Series-Fed Dual-Polarized Single-Layer Linear Patch Array With High Polarization Purity. *IEEE Antennas Wirel. Propag. Lett.* **2019**, *18*, 1746–1750.
18. Balanis, C.A. *Advanced Engineering Electromagnetics*; John Wiley & Sons: Hoboken, NJ, USA, 2012.
19. Deslandes, D.; Ke Wu. Accurate modeling, wave mechanisms, and design considerations of a substrate integrated waveguide. *IEEE Trans. Microw. Theory Tech.* **2006**, *54*, 2516–2526.
20. Wang, J. Measuring 3-Port Mixed-Mode S-Parameters. Available online: https://www.eetimes.com/measuring-3-port-mixed-mode-s-parameters-2/ (accessed on 22 January 2021).
21. Zou, X.; Geng, F.; Li, Y.; Leng, Y. Phase Inverters Based on Substrate Integrated Waveguide. *IEEE Microw. Wirel. Compon. Lett.* **2017**, *27*, 227–229.
22. Luo, Y.; Chen, Z.N.; Ma, K. A Single-Layer Dual-Polarized Differentially Fed Patch Antenna With Enhanced Gain and Bandwidth Operating at Dual Compressed High-Order Modes Using Characteristic Mode Analysis. *IEEE Trans. Antennas Propag.* **2020**, *68*, 4082–4087.